



Hydrochar and Value-Added Chemical Production Through Hydrothermal Carbonisation of Woody Biomass

Fatih Güleç^{1,2} * 

¹Low Carbon Energy and Resources Technologies research group, Faculty of Engineering, University of Nottingham, Nottingham, NG7 2TU, United Kingdom.

²Advanced Materials Research Group, Faculty of Engineering, University of Nottingham, Nottingham, NG7 2RD, United Kingdom.

Abstract: This study investigates the optimisation of hydrothermal carbonisation (HTC) parameters for transforming Whitewood biomass into hydrochar, focusing on bioenergy production and valuable chemical extraction as by-products. The optimal carbonisation was achieved at a process temperature of 240 -260 °C, which optimised the higher heating value of the hydrochar to 27-30 kJ/g and ensured a structural integrity similar to lignite coal. Increasing the temperature beyond 260 °C did not significantly enhance the energy content or quality of the hydrochar, establishing 260 °C as the practical upper limit for the HTC process. Residence times between 30 to 60 min were found to have minimal impact on the yield and quality of hydrochar, suggesting significant operational flexibility and the potential to double throughput without increasing energy consumption. The study also revealed that the process water by-product is rich in furan compounds, particularly furfural and hydroxymethyl furfural, with their highest concentration (125 mg/g of feedstock) occurring at 220 °C. The implementation of these findings could facilitate the development of a large-scale HTC facility, significantly reducing reliance on fossil fuels and enhancing economic viability by producing high-energy-density biofuels and high-value chemical by-products.

Keywords: Hydrothermal carbonisation, Biomass valorisation, Hydrochar, Value-added chemicals, Sustainable energy.

Submitted: May 15, 2024. **Accepted:** June 22, 2024.

Cite this: Güleç, F. (2024). Hydrochar and Value-Added Chemical Production Through Hydrothermal Carbonisation of Woody Biomass. *Journal of the Turkish Chemical Society, Section B: Chemical Engineering*, 7(2), 141-154. <https://doi.org/10.58692/jotcsb.1484204>.

***Corresponding author. E-mails:** Fatih.Gulec1@nottingham.ac.uk; Gulec.Fatih@outlook.com.

1. INTRODUCTION

The need for renewable energy sources has never been more critical. With an estimated 37.55 billion metric tonnes of CO₂ released into the atmosphere in 2023 (Tiseo, 2024). A rapid increase in global warming over the past few decades has brought the need for innovative, clean energy solutions. Many countries have been setting new policies and laws to reduce their Carbon Emissions and undo the near-irreversible consequences of global warming (Global CCS Institute, 2018). In 2019, the UK Government committed to achieve net zero by 2050. To meet this target, the UK signed an agreement at COP26 to end investments in new coal power generation (Smith et al., 2022; WHO, 2021). This follows the key policies in the Net Zero Strategy stating by 2035 the UK will be powered entirely by clean energy, subject to the security of supply (UK-Government, 2021).

The undeniable potential of biomass and bioenergy to replace fossil fuels in existing processes to produce heat, electricity, and fuel for transportation makes it an attractive and promising energy resource (Güleç, Samson, et al., 2022; Güleç, Williams, Kostas, Samson, et al., 2022). In order to valorise the biomass sources, there are many thermochemical processes such as hydrothermal conversion, pyrolysis, gasification and combustion. Hydrothermal Carbonisation (HTC) is an emerging thermochemical process that could be used in the bioenergy sector through the conversion of biomass into hydrochar (Sharma et al., 2020; Shen, 2020). Compared to other thermal conversion technologies i.e. pyrolysis or gasification, HTC is favourable (Bevan et al., 2021) as it does not require drying of the feedstock, which is highly energy-intensive and expensive.

The desired water content of the HTC feed is 75-90% (Kumar & Ankaram, 2019). Hydrochar obtained from HTC has been identified as a potential biofuel (Oumabady et al., 2020), contributing to this shift towards renewable energies and giving a major reason industries cite for not readily adopting biofuels is non-compatibility with existing equipment (Singh et al., 2022). Therefore, if it can be commercialised, HTC of biomass offers an attractive way to produce cleaner fuel for major industries, with the global biofuels arena growing at a rate of over 8% annually (Powell, 2022) and expected to surpass US\$200 billion in value by 2030. HTC can therefore provide an effective waste management system, and no ethical concerns arise from using second-generation biomass waste (Phang et al., 2023). Furthermore, hydrothermal conversion technologies including carbonisation, liquefaction, and gasification align well with Sustainable Development Goals (SDG7, SDG9, and SDG12) fostering cleaner energy solutions and promoting sustainable industrialisation and innovation (Welfle et al., 2023).

The selection of biomass feedstock and the parameters of the HTC process are crucial in ensuring that the resulting hydrochar meets the necessary specifications for its use as an industrial fuel. The presence of high-ash fuels can significantly increase fouling and slagging in combustion equipment, while alkaline metals in the ash may catalyse the combustion of hydrochars, altering their combustion characteristics compared to fossil coal (Stirling et al., 2018). Consequently, the ash content of the hydrochar must remain below 12 wt.% to meet industrial standards use (Agency, 2016). Due to their relatively low ash content and widespread availability, woody biomasses are particularly attractive feedstocks for HTC processes (Daskin et al., 2024). These woody feedstocks can be efficiently converted into hydrochar through HTC, making them a promising component in the production of green energy. Their global abundance and sustainable nature further enhance their appeal, as they help reduce reliance on non-renewable energy sources and contribute to the mitigation of environmental impacts associated with energy production.

This study focuses on the valorisation of Whitewood (WW) biomass using a lab-scale HTC reactor, aiming to produce sustainable hydrochar and value-added chemicals. Operating under a range of conditions, with temperatures between 200-280 °C and residence times from 30 to 180 min, the research includes a thorough characterisation of the solid, liquid, and gaseous products generated during the HTC process. The novelty of this research lies in its comprehensive evaluation of Whitewood biomass in the HTC process, assessing its applicability as a feedstock and identifying potential value-added products, including biochemicals, biogas, and hydrochar. Specifically, this paper presents the chemical composition and thermal properties of hydrochar to determine its suitability for bioenergy applications.

Additionally, it investigates the potential for extracting value-added chemicals from the liquid by-products through advanced chemical analyses. The study also assesses the gaseous products to understand their environmental impact and practical implications, thereby contributing comprehensive insights into the effectiveness and sustainability of the HTC process.

2. EXPERIMENTAL SECTION

A Whitewood (WW) Northern Ireland, supplied by Wolseley, was used as the biomass feedstock for the HTC process. The WW came in pellets formed from sawdust residues. The material was chosen due to its abundance and having been produced in the United Kingdom. To ensure the particle size was below 1 mm, the WW was milled in a Ball Mill for 2 min at 600 rpm. The milling process ensures homogeneity of the particles. Particle size can play a major role in heat and mass transfer within the HTC process. Larger particle sizes lead to slower reaction rates and incomplete conversion of the biomass. Smaller particle sizes are exposed to more water and heat, promoting hydrolysis and dehydration reactions.

2.1. Hydrothermal Carbonisation of Whitewood

The HTC experiments were carried out using a batch High-Pressure Autoclave Reactor System. WW sample (4.00 ± 0.01 g) was loaded into the vessel along with distilled water (26.00 ± 0.01 g) and mixed thoroughly to ensure homogeneity. The reactor vessel was sealed and flushed with nitrogen ensuring no air was present in the vessel, before being pressurised to 5 bar. A fluidised sand bed was then heated to the carbonisation temperature of 200 °C - 280 °C using compressed air entering at the bottom of the bed. When the sand-bed reach the set temperature, the autoclave was placed in the sand bed and kept at the isothermal temperature for a residence time of 30 min, 60 min, and 180 min. The temperature was monitored using an additional K-type thermocouple. Following the carbonisation, the reactor was moved to a separate cold fluidised sand bed maintained at 20 °C for 1 h to allow the vessel to cool down. After the elapsed hour a gas syringe was used to collect gaseous products whilst liquid and solid hydrochar was separated using a vacuum filtration unit. The primary products (solid, liquid, and gas) yields are calculated using Eq1-Eq3 (Güleç et al., 2021; Koechermann et al., 2018). Furthermore, hydrochar yield (Eq-4) is determined as the fixed carbon yield of the process. This is calculated by multiplying the fixed carbon content by the dry solid yield. Specifically, it involves assessing the proportion of fixed carbon in the hydrochar relative to the initial dry biomass, providing a clear measure of the efficiency and effectiveness of the hydrothermal carbonisation process in converting biomass to carbon-rich solid fuel.

$$\text{Solid yield (wt. \%)} = \frac{m_{\text{drychar}}}{m_{\text{ww},0}} * 100 \quad (1)$$

$$\text{Gas yield (wt. \%)} = \frac{m_{\text{gas}}}{m_{\text{ww},0}} * 100 \quad (2)$$

$$\text{Liquid yield (wt. \%)} = 100 - \text{Solid yield} - \text{Gas yield} \quad (3)$$

$$\text{Hydrochar yield (wt. \%)} = \left[\frac{m_{\text{drychar}}}{m_{\text{ww},0}} * 100 \right] * FC \quad (4)$$

Where, m_{drychar} ; represents the dry mass of solid char collected following the HTC process, $m_{\text{ww},0}$; represents the initial dry mass of feedstocks (ww), m_{gas} ; is the mass of the gas product collected following the HTC process (as determined by GC-MS analysis), FC is the fixed carbon content of hydrochar in wt.%.

2.2. Characterisation of Solid Hydrochar

2.2.1. Proximate analysis and thermal decomposition

Proximate analysis were performed by thermogravimetric analysis (TGA) using a TA-Q500 using a slow pyrolysis procedure presented before (Güleç et al., 2021; Lester et al., 2007). This method provides proximate analysis and enables further information regarding the changes in the composition of hydrochar by identification of displacement level. Approximately 30 mg of hydrochar was placed in a platinum pan of a model Q500 TGA. Samples were then heated from ambient temperature to 900 °C, at a heating rate of 5 °C/min, under a nitrogen flow of 100 mL/min. It was then held isothermally for 10 min to ensure total devolatilisation before changing the gas flow to 100 mL/min of air for 15 min to combust the fixed carbon. The temperature was then ramped down to 35 °C at a rate of 30 °C/min (Güleç et al., 2021; Lester et al., 2007). The mass loss before 110 °C was assumed to be moisture as the temperature is above the boiling point of water but below the temperature range for the thermal decomposition of hemicellulose, cellulose, and lignin. Mass loss from 110 °C up to 900 °C was considered volatile matter (VM) as the sample was under an inert nitrogen atmosphere. The rest of the mass loss was under airflow and considered as fixed carbon (FC). The remaining mass represented the ash content of the hydrochar. Three samples of feedstock and three hydrochars produced at the same process conditions were analysed to reduce systematic error.

2.2.2. Displacement

A novel characterisation property, suggested by (Lester et al., 2007), called "Displacement" has

been utilised to quantify the degree of hydrochar upgrade in HTC process using Eq 5. This dimensionless quantity provides a method to quantitatively compare the effectiveness of the hydrothermal treatment. It has been calculated from the absolute difference between the derivative weight loss from the feedstocks and the derivative weight loss from the hydrochar at each temperature, T.

$$\text{Displacement} = \sum_{T_i}^{T_f} \left(\left| \left(\frac{dw}{dt} \right)_{bf,T} \right| - \left(\frac{dw}{dt} \right)_{hc,T} \right) \quad (5)$$

Where, T_i and T_f are the temperature limits of the devolatilisation; 110°C and 900°C respectively. The higher the magnitude of displacement, the more structural decomposition has occurred during HTC process.

2.2.3. Ultimate Analysis

Ultimate (elemental) analysis was carried out for each hydrochar and feedstock using a Leco CHN628 and utilising helium as the carrier gas. Multiple pure standards of BBOT were used for calibration. Approximately 75 mg of sample was used per analysis. The oxygen content was determined by difference, assuming the total remaining was wholly elemental oxygen. The elemental analysis was triplicated to eliminate experimental error.

2.2.4. Fuel Characteristics

The higher heating value (HHV) of the hydrochars was estimated by a correlation with the ultimate analysis data (Callejón-Ferre et al., 2011). This particular correlation (Eq 6) was chosen based on a comprehensive analysis by (Daskin et al., 2024; Güleç, Williams, Kostas, Samson, et al., 2022) which showed that it had the lowest standard deviation from experimental data of 11 different theoretical correlations for the same feedstock.

$$\text{HHV} = -3.440 + 0.517(C+N) - 0.433(H+N) \quad (6)$$

Where, HHV is the higher heating value, C, N, and H are the elemental composition of Carbon, Nitrogen, and Hydrogen, respectively.

2.3. Characterisation of Process Liquid

Dichloromethane (DCM) was selected as the solvent to extract organic compounds for analysis from the process water by liquid-liquid extraction. It has mid-range polarity, meaning most organics will dissolve into it, plus DCM is immiscible with the water phase and denser, so can be easily drained off from a separating flask. Additionally, DCM is highly volatile, so it readily evaporates leaving behind the extracted compounds of interest. Extraction was performed by making 6 mL process water up to 15 mL volume with deionised water, then mixing with 15 mL DCM and settling for 5 min before draining off the solvent. This was repeated 3 times to extract maximum organics. The DCM was left to evaporate overnight, and a standard solution of squalane was prepared and 100 μ L added to each sample. Squalane is a hydrocarbon not found in the process liquid, so its peak in the gas chromatography (GC) output was used as a reference point to enable the quantification of all other compounds. The organic compounds were analysed on a 6850 Agilent HP GC connected to a 5975 Agilent HP quadrupole mass spectrometer (MS), (EI mode, 70 eV). GCMS was equipped with an autosampler and a split/splitless injector. Compounds were separated by a DB-1701 MS fused silica capillary column (60 m \times 0.25 mm i.d. \times 0.5 μ m film thickness) with helium as the carrier gas, and an oven program of 50 $^{\circ}$ C (held for 2 min) to 280 $^{\circ}$ C (held for 25 min), heated at a rate of 4 $^{\circ}$ C/min. MS is used for qualitative analysis, with compounds determined according to the NIST Mass Spectral Library from the National Institute of Standards and Technology, Maryland, USA. Compounds were then quantified with a Flame ionisation detector (FID). FID was used for quantification over MS as outputs are more reproducible and represent the composition of a mixture more reliably (St Gelais, 2014). This is because MS detects ions of fragmented compounds, with fragmentation and ionisation potential varying between compounds (Cicchetti et al., 2008), so is not suited to accurately measure the composition of a mixture. FID is inherently more quantitative as it works on the principle of detecting ions formed during the combustion of organic compounds.

2.4. Characterisation of Gas Products

Gas products were collected in an airtight bag and immediately analysed using Clarus 580 gas chromatography (GC) fitted with a Flame ionisation detector (FID) and thermal conductivity detector (TCD) operating at 200 $^{\circ}$ C. The gas samples were analysed by injecting 100 μ L of each gas sample (split ratio 10:1) into the GC at 250 $^{\circ}$ C with separation performed on an alumina plot fused silica 30 m \times 0.32 mm \times 10 μ m column, with helium as the carrier gas. The FID detector was used to analyse the hydrocarbon compounds and

TCD detector was used to analyse nonhydrocarbon compounds. The oven temperature was programmed from 60 $^{\circ}$ C (13 min hold) to 180 $^{\circ}$ C (10 min hold) at 10 $^{\circ}$ C/min.

3. RESULTS AND DISCUSSION

3.1. Hydrothermal Carbonisation of Whitewood

Figure 1 presents the yields of solid, liquid, gaseous primary products and hydrochar as functions of the hydrothermal carbonisation (HTC) process parameters: temperature (200 $^{\circ}$ C to 280 $^{\circ}$ C), residence time (30 to 180 min), and autogenous pressure, using biomass to water mass ratio of 1:6.5. The solid hydrochar product is generated through the decomposition and carbonisation of the major structural components of biomass—namely hemicellulose, cellulose, and lignin—which undergo hydrolysis, dehydration, and decarboxylation reactions. Specifically, the temperatures required to decompose these components range broadly, with hemicellulose starting to decompose at temperatures as low as 220 $^{\circ}$ C, cellulose at around 280 $^{\circ}$ C, and lignin between 160 $^{\circ}$ C and 900 $^{\circ}$ C (Güleç, Samson, et al., 2022; Güleç, Williams, Kostas, Samson, et al., 2022).

At lower temperatures (200–220 $^{\circ}$ C), the HTC process has a limited effect on the yield of solid hydrochar. The hydrochars produced at these temperatures exhibit only partial carbonisation, characterised by a light brown colour and large particle structure, similar to the original WW feedstock. These conditions result in less than 37 wt.% of the biomass being converted into gaseous and liquid products, indicating an incomplete carbonisation process. This is akin to findings by (Musa et al., 2022), where low temperatures were insufficient for the complete decomposition of major biomass components, such as Pine Kraft Lignin, leading to a higher yield of hydrochar. As the HTC temperature increases from 220 $^{\circ}$ C to 240 $^{\circ}$ C, there is a notable reduction in the yield of hydrochar from 64 wt.% to 49 wt.%, accompanied by an increase in the production of gaseous and liquid products. The hydrochars obtained at 240 $^{\circ}$ C are transformed into a homogeneous, blackish, coal-like solid structure. This decrease in hydrochar yield can be attributed to the major decomposition and carbonisation of hemicellulose within the feedstock, as this temperature range is ideal for hemicellulose breakdown but still below the decomposition temperatures for cellulose and lignin. Regarding residence time, Figure 1 shows a slight decrease in hydrochar yield from 65 wt.% to 59 wt.% as residence time increases from 30 to 180 min. Concurrently, the gas yield increases from 1 wt.% to 8 wt.%, corroborating findings by (Musa et al., 2022). (Ghanim et al., 2016) suggests that the increase in gas and liquid products at longer residence times could be explained by the degradation of soluble hemicellulose, cellulose, and lignin fragments in the aqueous phase.

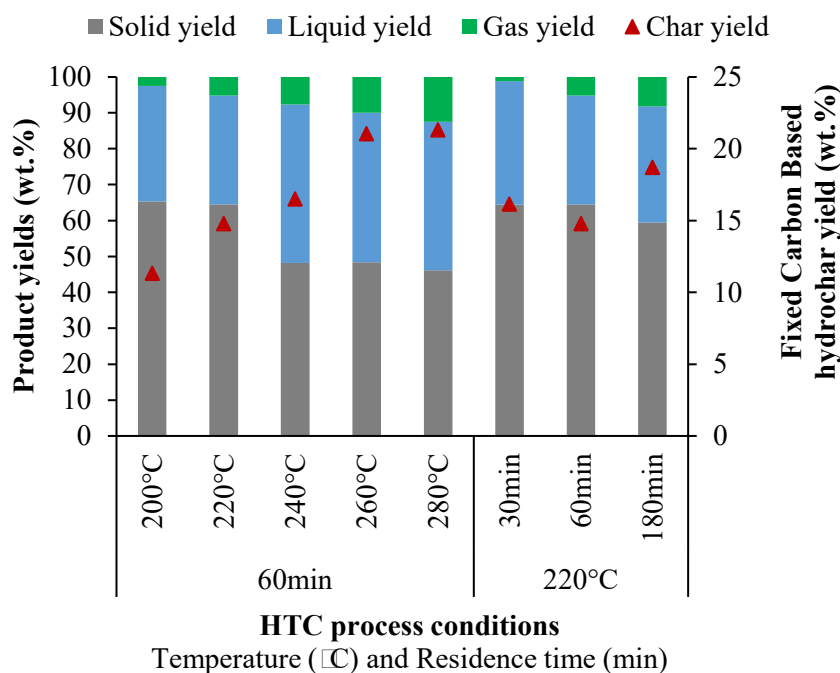


Figure 1. Solid (grey bar), liquid (blue bar), gaseous (green bar) and hydrochar (red triangle) product yields as a function of HTC process temperature (200 °C–280 °C), residence time (30–180 min) and autogenous pressure using biomass to water mass ratio of 1:6.5.

The linear increase in gas product yield across the experimental temperature range from 2.5 wt.% at 200 °C to 12.5 wt.% at 280 °C highlights a strong correlation between process temperature and gas yield. Although liquid product yield also increases from 30.3 wt.% to 49.6 wt.% as the temperature rises from 220 to 240 °C, further temperature increases do not significantly alter liquid yield, indicating that the majority of solid biomass decomposes primarily through liquefaction at these critical temperatures (220–240 °C). Figure 1 also shows that the fixed carbon-based hydrochar yield increases with rising process temperatures and residence times. For instance, at a constant residence time of 60 min, increasing the temperature from 200 °C to 260 °C results in a progressive increase in char yield from 11 wt.% to 21 wt.%. This indicates that higher temperatures facilitate the conversion of biomass into hydrochar, enhancing the carbon content. At 220 °C, increasing the residence time from 30 min to 180 min leads to a slight increase in hydrochar yield from 16 wt.% to 19 wt.%. This suggests that longer exposure to the HTC conditions promotes further carbonisation of the biomass, although the effect is less pronounced compared to temperature changes.

3.2. Fuel Characteristics of Hydrochars

3.2.1. Proximate analysis, Ultimate analysis, and HHV

Figure 2a illustrates the proximate analyses of feedstock and hydrochars. The fixed carbon ratio shows a notable increase from 17 wt.% to 44 wt.% as the hydrothermal temperature is raised from 200 °C to 280 °C. This increase in fixed carbon content correlates with a significant decrease in

volatile matter, which drops from 80 wt.% to 50 wt.%. While residence time does affect carbonisation, with fixed carbon increasing from 25 wt.% to 31 wt.% as residence time extends from 30 min to 180 min, the impact of residence time is substantially less significant than that of temperature (Güleç, Williams, Kostas, Samson, et al., 2022; Musa et al., 2022). The ultimate analysis results, as shown in Figure 2b, indicate that the carbon content of the biomass increases due to hydrothermal carbonisation. The increase in carbon content from 47 wt.% to 70 wt.% is more pronounced with higher process temperatures at 280 °C. Similarly, an increase in residence time also leads to a slight rise in carbon content from 54 wt.% to 60 wt.%, further emphasising the influence of temperature and residence time on the carbon yield in the hydrothermal carbonisation process.

Similar to the fixed carbon-based hydrochar yield (Figure 1), the HHV of solid products, as calculated and shown in Figure 2a, shows a considerable increase from 18 kJ/g to 30 kJ/g with the escalation of process temperature from 200 °C to 260 °C. In contrast, increasing the residence time from 30 min to 180 min at a constant temperature of 220 °C results in a smaller increase in HHV, from 22 kJ/g to 25 kJ/g. This suggests that temperature is a more critical factor than residence time in enhancing the energy content of hydrochars. Both hydrochar yield and HHV propose that optimising the temperature during the HTC process is crucial for maximising both the yield and energy content of hydrochar. Adjusting the residence time can further fine-tune these outcomes, but its effects are secondary to those of temperature.

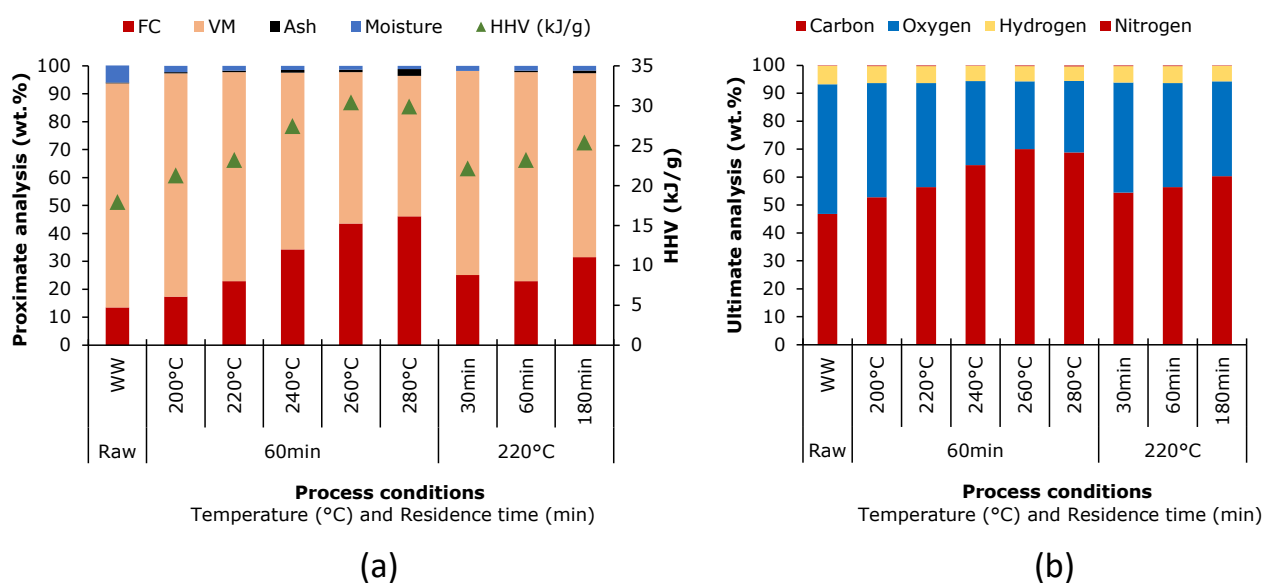


Figure 2. a) Proximate analysis and b) Ultimate analysis results of raw feedstocks and hydrochars produced with HTC (200°C–280°C, 30-180 min and autogenous pressure).

Additionally, ash content is a vital parameter for determining the suitability of hydrochar in energy production. Initial measurements showed the ash content in feedstock to be 0.23 wt.%. However, the hydrochars exhibited higher ash contents than the original feedstocks; this increase is due to a reduction in solid yield rather than an absolute increase in ash mass. Specifically, hydrochar produced at 200 °C had an ash content of 0.42 wt. %, which escalated to 2.42 wt.% at 280 °C, with a standard error of $\pm 0.32\%$. The HTC process tends to leech organic compounds into the process water, increasing the relative ash proportion in the solid residue, although the inorganic material is somewhat removed from the biomass (Hansen et al., 2020). Despite these increases, all samples

maintained an ash content well below the 12 wt.% thresholds considered acceptable for bioenergy applications, affirming that hydrochars produced from WW are suitable for use as fuel in green energy generation. The hydrochars in this study were produced in a batch process, which, compared to a semi-continuous HTC process involving WW, tends to result in 50 wt.% lower ash content (Güleç, Williams, Kostas, Smon, et al., 2022). This suggests that allowing process water to interact with the hydrochars during the reaction facilitates the transfer of inorganic material to the liquid phase, a crucial consideration for feedstocks intended for semi-continuous processing where slightly higher ash content might still be acceptable for combustion in industrial boilers.

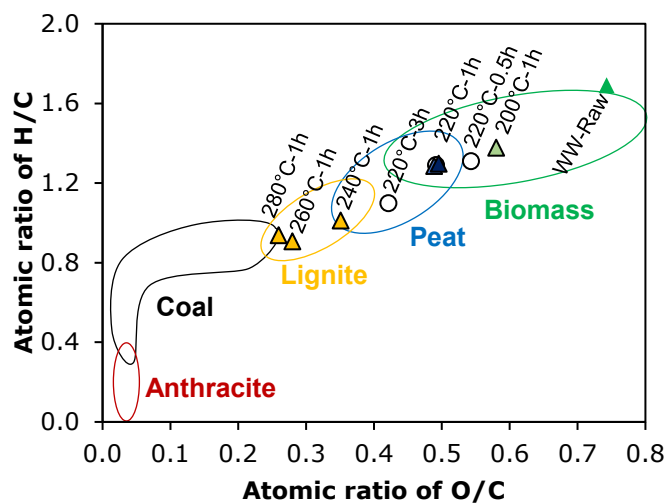


Figure 3. Van Krevelen diagram for raw biomass feedstocks (WW-Raw) and hydrochars produced as under HTC process conditions; 200°C–280°C, 30-180 min and autogenous pressure.

The Van Krevelen diagram (Figure 3), which plots the atomic ratio of H/C versus O/C, provides detailed insights into the fuel characteristics of produced hydrochars relative to conventional fuels such as peat, lignite, coal, and anthracite. The diagram shows the results of complex reactions including dehydration, demethylation, and decarboxylation, as noted by Güleç et al. (Güleç, Samson, et al., 2022; Güleç, Williams, Kostas, Samson, et al., 2022). Figure 3 indicates the trends, which is characterised by an increase in carbon content, leading to reduced atomic O/C and H/C ratios. This trend is a consistent dehydration pattern as both temperature and residence time increase. The dehydration process provides lower hydrogen and oxygen content within the hydrochar (Funke & Ziegler, 2010). The hydrochars produced at 200 and 220 °C are categorised within the Biomass zone, while those at 240 °C align with the Peat-Lignite zone, and those at 280 °C approach the border between Lignite-Coal. This progression demonstrates how increases in temperature progressively enhance the structure of the hydrochar, fostering a coal-like structure by carbonising biomass.

0.0.1. Thermal Decomposition and Displacement

Figure 4 shows the thermal decomposition and derivative weight changes during the slow pyrolysis of WW and hydrochars produced from WW. This analysis provides further details about the chemical composition of hydrochars following specific HTC processes. The degradation temperatures of biomass constituents are known as hemicellulose decomposes between 220-315 °C, cellulose between 315-400 °C, and lignin over a broad range of 160-900 °C (Yang et al., 2007).

The hydrous nature of HTC plays a crucial role in the process. Hydrolysis reactions, which predominantly involve the splitting of ester and ether bonds in biopolymers, lead to their breakdown into oligomers and monomers (Funke & Ziegler, 2010; Güleç et al., 2023). For instance, the disappearance of the hemicellulose shoulder in the raw WW observed in Figures 4b indicates that the hemicellulose structure can decompose at temperatures above 200 °C, a process that begins as low as 180 °C (Funke & Ziegler, 2010).

Significant peaks (260-340 °C) representing the cellulose-lignin structure remain in the hydrochars produced at 200 and 220°C. However, further carbonisation at higher temperatures, such as 240°C, leads to the breakdown of cellulose, as evidenced by the decrease in the cellulose-lignin peak shown in Figure 4b. Increasing the temperature further to 260 °C and 280 °C results in almost complete disappearance of this peak, indicating significant cellulose decomposition (Güleç et al., 2021). At the highest investigated temperatures, a new peak emerges at approximately 390-450 °C, correlating with the concentration of lignin remaining in the solid product.

The devolatilisation profiles of hydrochars produced at residence times of 30 and 180 min show more carbonisation than those processed for 60 min (Figure 4d). Interestingly, while the increased carbonisation at 180 min aligns with expectations due to prolonged reaction time, the similar profile at 30 min contradicts other studies that suggest longer times lead to more carbonisation (Cao et al., 2021; Reza et al., 2015; Smith & Ross, 2019). The unexpected trend in hydrochar produced at the residence time of 30 min and 60 min can be attributed to the cooling time. In these experiments, the cooling period lasts approximately one hour, which is longer than the actual residence times of 30 min and equal to 60 min, resulting in a total process time of 90-120 minutes from heating to cooling. This prolonged cooling period effectively extends the carbonisation process, reducing the differences between hydrochars produced at these shorter residence times. Given that the impact of residence time has shown minimal enhancement in the hydrochar (Figure 1-3), it is likely that the differences observed between the 30 min and 60 min conditions are due to the short residence time of the process rather than a consistent experimental trend. (Smith & Ross, 2019) found that temperature has a more significant impact on hydrochar characteristics than residence time. In order to enhance the understanding of short residence time, further investigation into the thermal dynamics and reaction kinetics during the cooling phase could provide deeper insights.

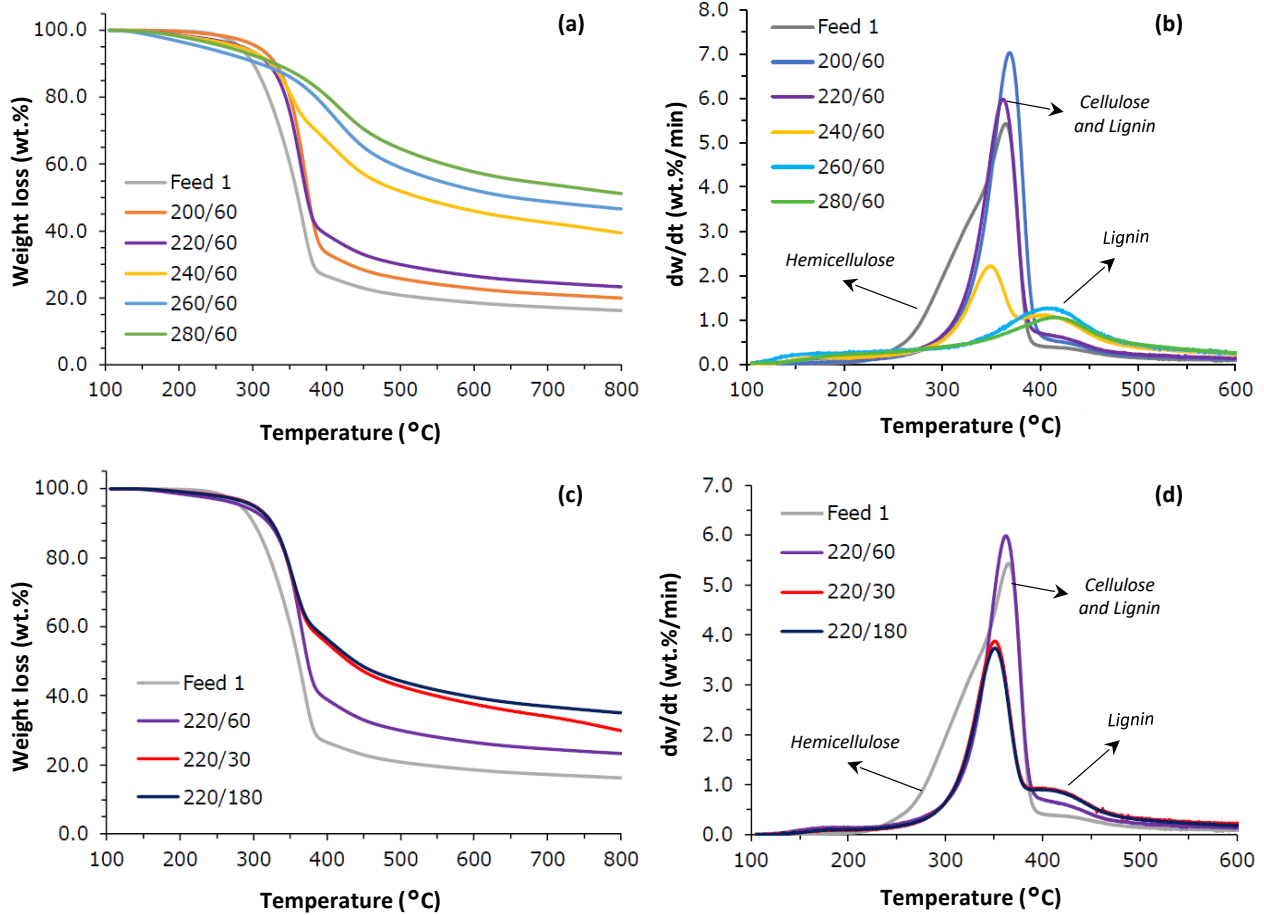


Figure 4. Thermal decomposition of WW and hydrochars under slow pyrolysis conditions (5 °C/min) and derivative weight change by temperature for a-b) hydrochars produced at different temperatures (200-280 °C) and c-d) hydrochars produced by different residence time (30-180 min).

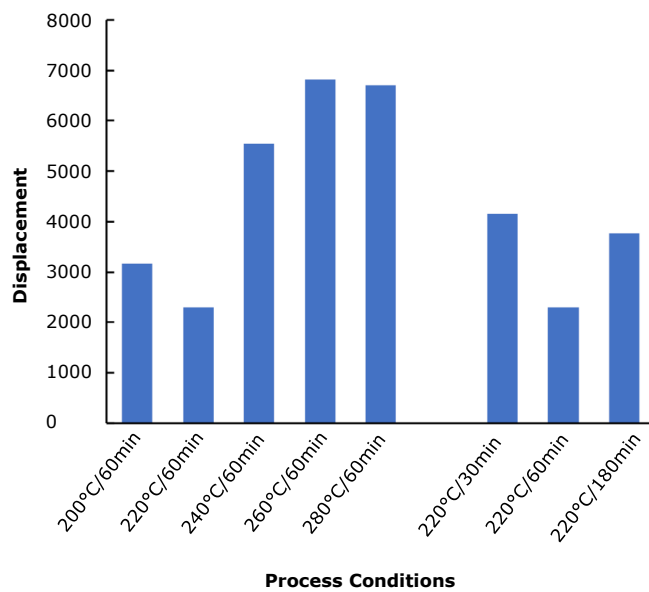


Figure 5. Displacement level of hydrochars produced at different temperatures (200-280 °C) and residence times (30-180 min).

Figure 5 shows the displacement levels of hydrochars across various temperatures and residence times. At elevated temperatures of 240 °C, 260 °C, and 280 °C, the displacement levels were notably high, ranging from 6000 to 7000, in stark contrast to the significantly lower displacement levels at elevated temperatures of 240 °C, 260 °C, and 280 °C.

displacements of 2000 to 3000 recorded at 200 °C and 220 °C. These substantial displacements at higher temperatures correspond with the notable absence of hemicellulose and cellulose in the devolatilisation profiles, which significantly contribute to the deviation in mass loss from the feedstock. However, it is interesting to note that the displacements at 220 °C were unexpectedly lower than those at 200 °C. Although higher displacement is generally favorable for achieving a better hydrochar structure, this is not always the case, particularly when biomass decomposes completely during the hydrothermal process. For instance, during hydrothermal gasification, biomass may transform into inorganic compounds, resulting in no char formation at the end of the reaction. This process might theoretically yield the maximum displacement, yet it does not necessarily indicate that the resulting material has desirable fuel properties. This suggests that displacement cannot be directly correlated with fuel quality based solely on displacement measurements.

3.3. Value-added Chemicals in Liquid Products

Figure 6 illustrates the various compounds present in the process water and the relative amounts between samples from HTC runs under varying conditions. It is seen that the largest peak at 19 min residence time, a furan compound, is only present in process liquid from HTC at the lowest temperatures of 200 °C and 220 °C, and is also not present in the liquid when residence time was only

30 min. The next most intense peak at 39 min is not present at all in the liquid from the hottest HTC run at 280 °C, and is noticeably less intense at 260 °C, whilst several other compounds are detected in these two samples which are not present in the process liquids from HTC runs at reduced temperatures.

The chemicals identified in the process liquid were categorised into four groups: Acids, Aldehydes & Ketones, Furans, and Phenols. Table 1 shows that the organic group generally present in the highest quantity in the process water is furans. Across all samples, the total amount of organics in the process water is highest for the HTC run at 220 °C and a 60 min residence time. Furans are the most prominent chemical group found in the process water by-product when HTC is carried out at 240 °C and below, and residence time is seen to have minimal impact on the quantities of furans present. Within this group, the main compounds are furfural and hydroxymethyl furfural (HMF). Furfural is typically generated from lignocellulosic biomass such as WW (Zhang et al., 2022). The high furfural content seen in liquid from lower temperature hydrochars supports later findings in this research that HTC does not decompose cellulose structures when the reaction occurs below 240 °C. Higher hydrochar processing temperatures likely caused furfurals to be decomposed into other molecules (Diaz Perez et al., 2023), as is seen by the numerous peaks representing compounds only present in the liquid from HTC at 280 °C.

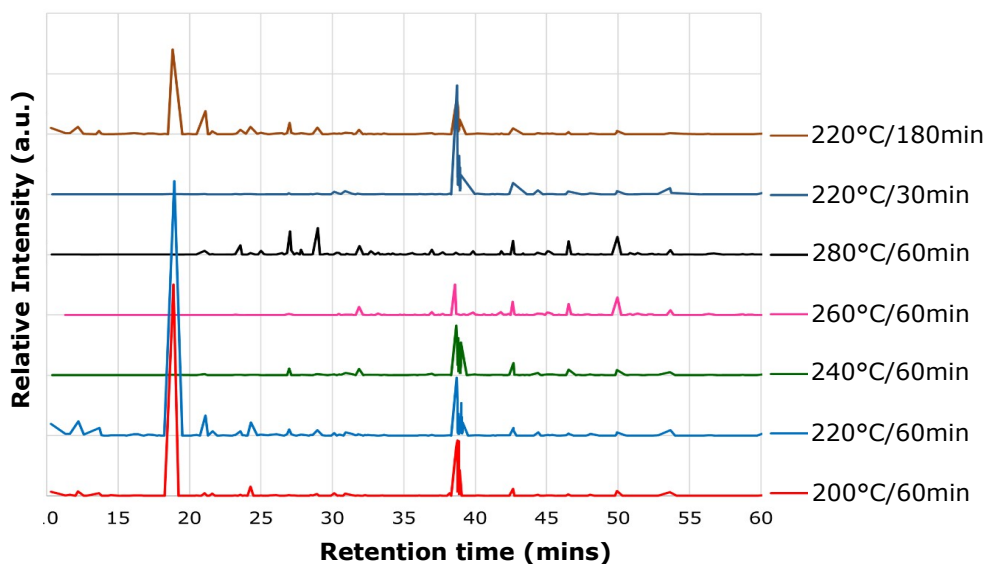


Figure 6. Relative peak intensities for liquid samples of the HTC process at different temperatures (200-280 °C) and residence times (30-180 min) (detailed peak definition is provided in Appendix A).

Table 1. Comparison of process liquid from HTC runs under varying temperatures and residence time.

| Value-added chemical compounds | Liquid Samples* | | | | | | 220°C 180mi n |
|---|--|-----------|-----------|-----------|-----------|------------------------|---------------------|
| | 200° C | 220° C | 240° C | 260° C | 280° C | 220° C 30mi n | |
| | 60min (mg/g Biomass Feedstock ±0.19 mg/g) | | | | | | |
| Acids | | | | | | | |
| Acetic Acid | 0.00 | 1.91 | 0.00 | 0.00 | 0.00 | 0.00 | 1.16 |
| Aldehydes & Ketones | | | | | | | |
| Acetol | 0.57 | 2.36 | 0.00 | 0.00 | 0.00 | 0.00 | 1.40 |
| Acetoin | 0.34 | 1.26 | 0.00 | 0.00 | 0.05 | 0.00 | 0.58 |
| Butanone | 0.30 | 3.37 | 0.19 | 0.00 | 0.59 | 0.00 | 4.42 |
| Hexanedione (Diacetyethane) | 0.00 | 0.70 | 0.00 | 0.00 | 1.40 | 0.00 | 0.81 |
| Corylone (Hydroxy Methyl Cyclopentenone) | 0.00 | 1.00 | 1.06 | 0.17 | 3.47 | 0.179 | 2.15 |
| Vanillin (Hydroxy Methoxy Benzaldehyde) | 0.87 | 2.11 | 1.92 | 1.83 | 2.07 | 1.696 | 1.11 |
| Total Aldehydes & Ketones | 2.08 | 10.80 | 3.17 | 2.00 | 7.57 | 1.87 | 10.48 |
| Furans | | | | | | | |
| Furfural | 26.49 | 42.39 | 0.00 | 0.00 | 0.05 | 0.00 | 16.36 |
| Ethanone (Furanyl) | 0.26 | 0.70 | 0.00 | 0.00 | 0.09 | 0.00 | 0.52 |
| Methyl Furaldeyde | 1.13 | 2.16 | 0.00 | 0.00 | 0.23 | 0.00 | 1.40 |
| Furyl Hydroxy Methyl Ketone | 0.34 | 0.40 | 0.14 | 0.17 | 0.32 | 0.40 | 0.12 |
| Furandicarboxaldehyde | 0.26 | 1.00 | 0.34 | 0.00 | 0.00 | 0.49 | 0.23 |
| Hydroxymethyl Furfural | 34.39 | 78.86 | 53.84 | 4.43 | 0.32 | 60.87 | 36.79 |
| | | 125.5 | | | | | |
| Total Furans | 62.89 | 2 | 54.32 | 4.60 | 0.99 | 61.77 | 55.42 |
| Phenols | | | | | | | |
| Methoxy Phenol | 0.00 | 0.90 | 0.19 | 0.00 | 3.96 | 0.00 | 1.22 |
| Methoxy Propyl Phenol | 0.15 | 0.55 | 0.38 | 0.21 | 0.32 | 0.58 | 0.00 |
| Hydroxy Methoxy Phenyl Propanone | 0.19 | 0.65 | 0.86 | 1.53 | 1.98 | 0.45 | 0.76 |
| Hydroxy Methoxy Phenyl Butanone | 0.11 | 0.25 | 0.14 | 0.00 | 0.00 | 0.18 | 0.00 |
| Hydroxy Methoxy Phenyl Propanol | 0.60 | 0.90 | 0.82 | 2.47 | 2.66 | 0.80 | 0.99 |
| Hydroxy Methoxy Phenyl Propanal | 0.87 | 0.90 | 0.48 | 0.68 | 0.68 | 0.94 | 0.00 |
| Total Phenols | 1.93 | 4.17 | 2.88 | 4.90 | 9.60 | 2.95 | 2.97 |

*Amounts of organic compounds are presented in milligrams per gram of WW feedstock. Error is calculated from the standard deviation of analysis results repeated for the 220°C 1 hour liquid sample and is found to be ± 0.19 mg/g, giving high confidence in the results.

Furfural has been used as a chemical feedstock in synthesising plastics, solvents, and resins, and it has been proven that furfural and HMF can be generated from biomass in high quantities at low cost (Siddarth H. Krishna, 2018). The global furfural market is valued around US\$600 million in 2023 (Statista, 2023) and is growing due to rising demand for sustainably produced chemical feedstocks for plastics. The combination of HTC conditions producing the highest quantity of furans in the process liquid at 125 mg per gram of WW feedstock is 220°C and 60 min residence time. This translates to 1 g of furans (primarily furfural and HMF) in the process liquid for every 8 g of WW that undergoes HTC. This relatively large amount of furfural and HMF is a key finding with major impacts to HTC process economics, given furfural can be expected to sell for US\$1000/tonne (Siddarth H. Krishna, 2018).

The next most prevalent chemical group is phenols. These are present in small quantities of <10 mg/g feedstock, and changes to HTC process conditions are not seen to correlate with a large change in phenolics, suggesting quantities are

more dependent on the biomass chosen for HTC rather than process parameters. Studies have shown HTC can be integrated with anaerobic digestors producing biogas (Brown et al., 2020) by using the process liquid as feedstock, however, phenols inhibit methane production when present in quantities greater than 1.5mg/L (Poirier & Chapleur, 2018). The process liquid from WW HTC is also suitable for use as a feedstock to anaerobic digestors, as total phenol levels are far below inhibiting limits, as shown in Table 1.

3.4. Gas Products

Figure 7 shows the composition of gaseous products generated during HTC at temperatures of 220 °C and 240 °C. Gas chromatography analysis reveals that the predominant component of the gaseous products at both temperatures is CO₂. Specifically, at 220 °C, three repeated gas analyses yielded an average CO₂ composition of 98 \pm 2.5 vol. %, with a 95% confidence interval. As the temperature of the HTC process increases, the volume fraction of CO₂ in the gas slightly decreases, while there is a noticeable increase in carbon monoxide (CO) production. At 240 °C, CO₂

and CO account for 92 vol.% and 7.11 vol.%, respectively. Additionally, there are minor increases in methane (0.1 vol.%), hydrogen (0.3 vol.%), and trace quantities of light hydrocarbons such as ethene and butene. This finding aligns with and is supported by results from a study by (Musa et al., 2022), which identified that the primary component of the gaseous phase product from HTC is CO₂, accompanied by some CO and trace amounts of hydrocarbon gases. Further quantitative comparisons can be made with a study by Basso et al., which provides additional insights into the composition of these gases (Basso et al., 2018).

While the gaseous products from HTC are not typically considered high-value, modifications to

the facility design could leverage these by-products effectively. For instance, recycling the gases produced back into the HTC reactor vessel could gradually increase the concentration of the gas product, resulting in a stream rich in CO₂, CO, H₂, and hydrocarbons. This enriched stream presents some utilisation options such as fuel source or carbon capture. If the concentration of hydrocarbons is sufficiently high, this stream could potentially be used as a fuel source, thereby reducing the energy demands of the HTC facility. Predominantly consisting of CO₂, this stream could be purified into a highly concentrated CO₂ stream, which could then be used in carbon capture and storage applications, contributing to the creation of carbon-negative bioenergy fuel.

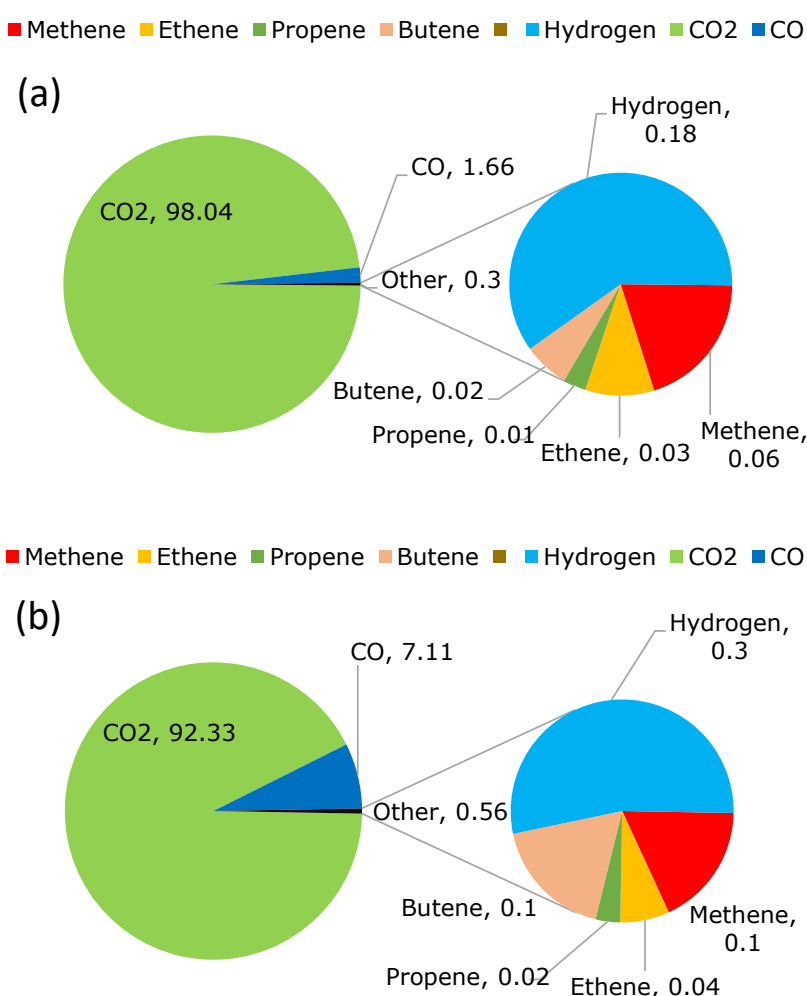


Figure 7. Gas composition (vol%) within the gaseous products of HTC process at the temperatures of a) 220°C and 60 min and b) 240°C and 60min.

4. CONCLUSION

This study systematically evaluated the optimisation of hydrothermal carbonisation (HTC) parameters for the production of hydrochar from woody biomass (whitewood), aimed at enhancing its suitability for bioenergy and value-added chemical applications. The findings show that a process temperature of 240-260 °C is optimal for

achieving effective carbonisation, maximising the higher heating value (27-30 kJ/g), and ensuring the structural integrity of the hydrochar similar to lignite-coal structure. Temperatures exceeding 260 °C do not yield significant improvements in the energy content or quality of the hydrochar, indicating that 260 °C is the upper limit for process temperature. Residence time has a minimal impact

on the yield and quality of hydrochar between 30 min to 60 min, allowing for operational flexibility and increased throughput without additional energy costs. The study also highlighted the importance of managing residence times to balance energy use with production efficiency. The process water by-product contains substantial quantities of furan compounds, specifically furfural and hydroxymethyl furfural. These compounds are most abundant when the HTC process is conducted at temperatures of 240 °C or lower. Optimal production of furans, reaching as high as 125 mg/g of feedstock, occurs at a temperature of 220 °C. Implementing the findings from this study could lead to the development of a large-scale HTC facility that not only contributes to reducing dependency on fossil fuels but also supports the economic viability through the production of both high-energy-density biofuels and valuable chemical by-products. This aligns with Sustainable Development Goals (SDG7, SDG9, and SDG12) fostering cleaner energy solutions and promoting sustainable industrialisation and innovation.

5. CONFLICT OF INTEREST

The authors have no conflict of interest.

6. ACKNOWLEDGMENTS

This research was partially funded and supported by the EPSRC, BBSRC and UK SuperGen Bioenergy Hub [Grant number EP/S000771/1], the University of Nottingham FPVC Research Acceleration Fund (Dr Fatih Gulec).

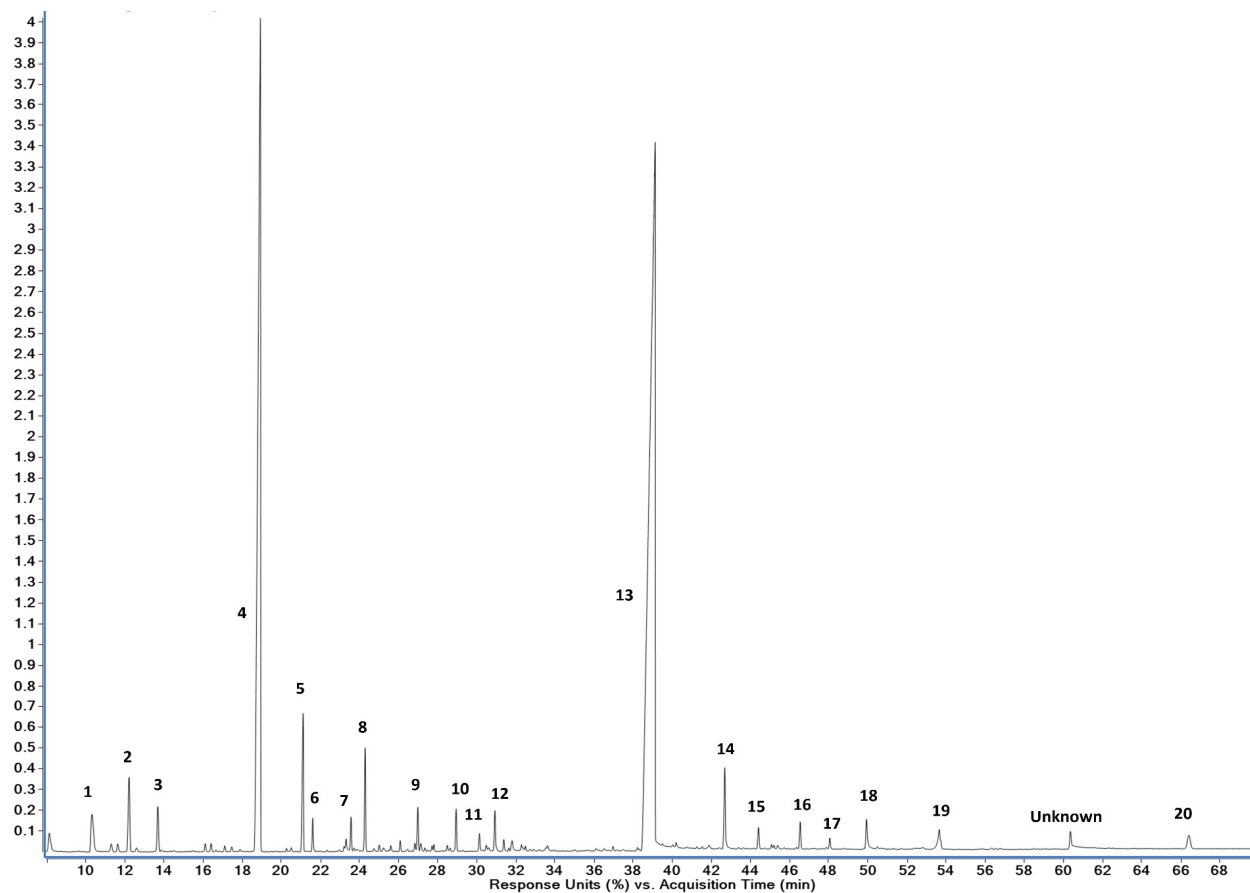
7. REFERENCES

- Agency, E. (2016). Material comparators for end-of-waste decisions.
- Basso, D., Weiss-Hortala, E., Patuzzi, F., Baratieri, M., & Fiori, L. (2018). In deep analysis on the behavior of grape marc constituents during hydrothermal carbonization. *Energies*, 11(6), 1379.
- Bevan, E., Fu, J., Luberti, M., & Zheng, Y. (2021). Challenges and opportunities of hydrothermal carbonisation in the UK; case study in Chirnside. *RSC advances*, 11(55), 34870-34897.
- Brown, A. E., Finnerty, G. L., Camargo-Valero, M. A., & Ross, A. B. (2020). Valorisation of macroalgae via the integration of hydrothermal carbonisation and anaerobic digestion. *Bioresource Technology*, 312, 123539.
- Callejón-Ferre, A., Velázquez-Martí, B., López-Martínez, J., & Manzano-Agugliaro, F. (2011). Greenhouse crop residues: Energy potential and models for the prediction of their higher heating value. *Renewable and Sustainable Energy Reviews*, 15(2), 948-955.
- Cao, Z., Hülsemann, B., Wüst, D., Oechsner, H., Lautenbach, A., & Kruse, A. (2021). Effect of residence time during hydrothermal carbonization of biogas digestate on the combustion characteristics of hydrochar and the biogas production of process water. *Bioresource technology*, 333, 125110.
- Cicchetti, E., Merle, P., & Chaintreau, A. (2008). Quantitation in gas chromatography: usual practices and performances of a response factor database. *Flavour and fragrance journal*, 23(6), 450-459.
- Daskin, M., Erdoğan, A., Güleç, F., & Okolie, J. A. (2024). Generalizability of empirical correlations for predicting higher heating values of biomass. *Energy Sources, Part A: Recovery, Utilization, and Environmental Effects*, 46(1), 5434-5450.
- Diaz Perez, N., Lindfors, C., A. M. van den Broek, L., van der Putten, J., Meredith, W., & Robinson, J. (2023). Comparison of bio-oils derived from crop digestate treated through conventional and microwave pyrolysis as an alternative route for further waste valorization. *Biomass Conversion and Biorefinery*, pp.1-16.
- Funke, A., & Ziegler, F. (2010). Hydrothermal carbonization of biomass: A summary and discussion of chemical mechanisms for process engineering. *Biofuels, Bioproducts and Biorefining*, 4(2), 160-177.
- Ghanim, B. M., Pandey, D. S., Kwapinski, W., & Leahy, J. J. (2016). Hydrothermal carbonisation of poultry litter: Effects of treatment temperature and residence time on yields and chemical properties of hydrochars. *Bioresource technology*, 216, 373-380.
- Global CCS Institute. (2018). The global status of CCS. <https://www.globalccsinstitute.com/resources/global-status-report/>
- Güleç, F., Parthiban, A., Umenweke, G. C., Musa, U., Williams, O., Mortezaei, Y., Suk-Oh, H., Lester, E., Ogbaga, C. C., & Gunes, B. (2023). Progress in lignocellulosic biomass valorization for biofuels and value-added chemical production in the EU: A focus on thermochemical conversion processes. *Biofuels, Bioproducts and Biorefining*, 18(3), 755-781.
- Güleç, F., Riesco, L. M. G., Williams, O., Kostas, E. T., Samson, A., & Lester, E. (2021). Hydrothermal conversion of different lignocellulosic biomass feedstocks–Effect of the process conditions on hydrochar structures. *Fuel*, 302, 121166.
- Güleç, F., Samson, A., Williams, O., Kostas, E. T., & Lester, E. (2022). Biofuel characteristics of chars produced from rapeseed, whitewood, and seaweed via thermal conversion technologies–Impacts of feedstocks and process conditions. *Fuel Processing Technology*, 238, 107492.
- Güleç, F., Williams, O., Kostas, E. T., Samson, A., & Lester, E. (2022). A comprehensive comparative study on the energy application of chars produced from different biomass feedstocks via hydrothermal conversion, pyrolysis, and torrefaction. *Energy Conversion and Management*, 270, 116260.
- Güleç, F., Williams, O., Kostas, E. T., Smon, A., & Lester, E. (2022). A comprehensive comparative study on the energy application of chars produced from different biomass feedstocks via hydrothermal conversion, pyrolysis, and torrefaction. *Energy Conversion and Management*, 270, 116260.

- Hansen, L. J., Fendt, S., & Spliethoff, H. (2020). Impact of hydrothermal carbonization on combustion properties of residual biomass. *Biomass Conversion and Biorefinery*, 12(7), 2541-2552.
- Koechermann, J., Goersch, K., Wirth, B., Muehlenberg, J., & Klemm, M. (2018). Hydrothermal carbonization: Temperature influence on hydrochar and aqueous phase composition during process water recirculation. *Journal of Environmental Chemical Engineering*, 6(4), 5481-5487.
- Kumar, S., & Ankaram, S. (2019). Waste-to-energy model/tool presentation. In *Current developments in biotechnology and bioengineering* (pp. 239-258). Elsevier.
- Lester, E., Gong, M., & Thompson, A. (2007). A method for source apportionment in biomass/coal blends using thermogravimetric analysis. *Journal of Analytical and Applied Pyrolysis*, 80(1), 111-117.
- Musa, U., Castro-Díaz, M., Uguna, C. N., & Snape, C. E. (2022). Effect of process variables on producing biocoals by hydrothermal carbonisation of pine Kraft lignin at low temperatures. *Fuel*, 325, 124784.
- Oumabady, S., Kamaludeen, S., Ramasamy, M., Kalaiselvi, P., & Parameswari, E. (2020). Preparation and Characterization of Optimized Hydrochar from Paper Board Mill Sludge. *Scientific reports*, 10(1), 773.
- Phang, F. J. F., Soh, M., Khaerudini, D. S., Timuda, G. E., Chew, J. J., How, B. S., Loh, S. K., Yusup, S., & Sunarso, J. (2023). Catalytic wet torrefaction of lignocellulosic biomass: An overview with emphasis on fuel application. *South African Journal of Chemical Engineering*, 43(1), 162-189.
- Poirier, S., & Chapleur, O. (2018). Inhibition of anaerobic digestion by phenol and ammonia: Effect on degradation performances and microbial dynamics. *Data in brief*, 19, 2235-2239.
- Powell, H. (2022). Biofuels market size to surpass \$201.21 billion by 2030. *Connected Energy Solutions*. <https://connectedenergysolutions.co.uk/biofuels-market-size-to-surpass-201-21-billion-by-2030/>
- Reza, M. T., Mumme, J., & Ebert, A. (2015). Characterization of hydrochar obtained from hydrothermal carbonization of wheat straw digestate. *Biomass Conversion and Biorefinery*, 5, 425-435.
- Sharma, R., Jasrotia, K., Singh, N., Ghosh, P., Sharma, N. R., Singh, J., Kanwar, R., & Kumar, A. (2020). A comprehensive review on hydrothermal carbonization of biomass and its applications. *Chemistry Africa*, 3(1), 1-19.
- Shen, Y. (2020). A review on hydrothermal carbonization of biomass and plastic wastes to energy products. *Biomass and Bioenergy*, 134, 105479.
- Siddarth H. Krishna, K. H., Kevin J. Barnett, Jiayue He, Christos T. Maravelias, James A. Dumesic, George W. Huber, Mario De bruyn, Bert M. Weckhuysen. (2018). Oxygenated commodity chemicals from chemo-catalytic conversion of biomass derived heterocycles. Department of Chemical and Biological Engineering, University of Wisconsin-Madison.
- Singh, A., Gill, A., Lim, D. L. K., Kasmaruddin, A., Miri, T., Chakrabarty, A., Chai, H. H., Selvarajoo, A., Massawe, F., Abakr, Y. A., & al., e. (2022). Feasibility of Bio-Coal Production from Hydrothermal Carbonization (HTC) Technology Using Food Waste in Malaysia. *Sustainability*, 14(8), 4534.
- Smith, A. M., & Ross, A. B. (2019). The influence of residence time during hydrothermal carbonisation of miscanthus on bio-coal combustion chemistry. *Energies*, 12(3), 523.
- Smith, P., Beaumont, L., Bernacchi, C. J., Byrne, M., Cheung, W., Conant, R. T., Cotrufo, F., Feng, X., Janssens, I., & Jones, H. (2022). Essential outcomes for COP26.
- St Gelais, A. (2014). GC Analysis – Part V. FID or MS for Essential Oils? *Laboratoire PhytoChemia*. <https://phytochemia.com/en/2014/09/02/gc-analysis-part-v-fid-or-ms-for-essential-oils/#:~:text=In%20general%2C%20the%20MS%20should,compound%20in%20an%20essential%20oil>
- Statista. (2023). Market value of furfural worldwide from 2015 to 2021, with a forecast for 2022 to 2029. <https://www.statista.com/statistics/1310467/furfural-market-value-worldwide/#:~:text=In%202021%2C%20the%20market%20of,566%20million%20U.S.%20dollars%20worldwide>
- Stirling, R. J., Snape, C. E., & Meredith, W. (2018). The impact of hydrothermal carbonisation on the char reactivity of biomass. *Fuel processing technology*, 177, 152-158.
- Tiseo, I. (2024). Annual carbon dioxide (CO₂) emissions worldwide from 1940 to 2023. Retrieved 13/05/2024 from <https://www.statista.com/statistics/276629/global-co2-emissions/>
- UK-Government. (2021). Net Zero Strategy: Build Back Greener.
- Welfle, A. J., Almena, A., Arshad, M. N., Banks, S. W., Butnar, I., Chong, K. J., Cooper, S. G., Daly, H., Freitas, S. G., & Güleç, F. (2023). Sustainability of bioenergy-Mapping the risks & benefits to inform future bioenergy systems. *Biomass and Bioenergy*, 177, 106919.
- WHO. (2021). COP26 special report on climate change and health: the health argument for climate action. World Health Organization.
- Yang, H., Yan, R., Chen, H., Lee, D. H., & Zheng, C. (2007). Characteristics of hemicellulose, cellulose and lignin pyrolysis. *Fuel*, 86(12-13), 1781-1788.
- Zhang, X., Zhu, P., Li, Q., & Xia, H. (2022). Recent Advances in the Catalytic Conversion of Biomass to Furfural in Deep Eutectic Solvents. *Frontiers in Chemistry*, 10, 911674.

APPENDICES

Appendix A: Labelled FID spectra with 20 main peaks identified in the table.



| Peak No | Molecular Mass (g/mol) | Compound Group | Compound Name |
|---------|------------------------|-----------------|--|
| 1 | 60 | Carboxylic Acid | Acetic Acid |
| 2 | 74 | Ketone | Acetol |
| 3 | 88 | Ketone | Acetoin |
| 4 | 96 | Furan | Furfural |
| 5 | 72 | Ketone | Butanone |
| 6 | 110 | Furan | Ethanone (Furanyl) |
| 7 | 114 | Ketone | Hexanedione (Diacetyethane) |
| 8 | 110 | Furan | Methyl Furaldeyde |
| 9 | 112 | Ketone | Corylone (Hydroxy Methyl Cyclopentenone) |
| 10 | 124 | Phenol | Methoxy Phenol |
| 11 | 126 | Furan | Furyl Hydroxy Methyl Ketone |
| 12 | 124 | Furan | Furandicarboxaldehyde |
| 13 | 126 | Furan | Hydroxy Methyl Furfural |
| 14 | 152 | Aldehyde | Vanillin (Hydroxy Methoxy Benzaldehyde) |
| 15 | 166 | Phenol | Methoxy Propyl Phenol |
| 16 | 180 | Phenol | Hydroxy Methoxy Phenyl Propanone |
| 17 | 194 | Phenol | Butyrovanilone (Hydroxy Methoxy Phenyl Butanone) |
| 18 | 182 | Phenol | Hydroxy Methoxy Phenyl Propanol |
| 19 | 178 | Phenol | Hydroxy Methoxy Phenyl Propanal |
| 20 | 196 | Alkane | Squalane (Reference Compound) |